Proceeding of the 2004 American Control Conference
Boston, Massachusetts June 30 - July 2, 2004

Human Thermal Model with Extremities for Asymmetric Environments

Anthony E. Iyoho, Tai S. Jang, and Satish S. Nair, *Member, IEEE*

Abstract - **A new human thermal model is developed that accounts for asymmetric environments and includes extremities. The model incorporates 2-dimensional (radial and circumferential) heat transfer along with arterial and venous countercurrent blood flow. Digits to predict toe and fingertip are modeled as arteriovenous anastomoses (AVAs), all of which are important in extremity discomfort.**

I. INTRODUCTION

NASA found during the first space flight that sufficient cooling of an astronaut could not be accomplished via air convection in the suit due to ventilation, and have since been using a liquid cooling garment (LCG) to circulate water for cooling the astronaut during space walks. In the present arrangement, the astronaut controls the temperature of the water flowing through the LCG by manually adjusting the temperature control valve (TCV) located on the front of the space suit. However, manually manipulating the TCV setting can dramatically reduce the productivity of the astronaut, distracting them from the extra-vehicular activity (EVA) mission at hand. In general, humans are poor judges of their thermal state and since an astronaut's attention is focused on other things during EVA, there are time lags in the application of temperature control. This can cause overheating or overcooling; placing unneeded thermal stress on the astronaut, and possibly degrading EVA performance. An attractive solution to this problem is the use of automatic control for thermal comfort. Before an automatic controller can be designed, human thermal models are needed to accurately describe the transient heat transfer processes and predict the thermal response within an acceptable band of accuracy. Such human thermal models can also be extended to handle various applications involving fire fighters, combat pilots, hazardous waste workers, and other industries where comfort in a thermally stressful environment needs to be insured.

The development of mathematical models for human thermoregulation started in the early 20th century. Early models used simple representations for the human thermal system, as it was not known of how much detail was needed to insure accuracy. However, in the 1960s, more detailed models surfaced as researchers strived to incorporate the complexities of human thermoregulation, as these complexities became known, to improve accuracy. Still the human thermoregulatory system, with its active and passive components, is difficult to model. Many aspects of the human's active thermal system are still not understood at all. The passive thermal system has been modeled with more success, but still uncertainties are present.

This paper shows in detail the aspects needed for the development of a human thermal model for extra-vehicular activity (EVA) applications in space. The paper includes: (i) a review of human thermal modeling, (ii) model additions to the 41-Node Man [1], (iii) dynamic equations for numerical solutions, and (iv) simulation results.

II. REVIEW OF HUMAN THERMAL MODELS

Numerous human thermal models have been developed and used in many practical applications for the past sixty years, starting with the development of a steady-state model to analyze heat transfer in a resting human forearm by Pennes in 1948 [2]. This cylindrical model served as the basis for a more advanced model by Wissler [3] and it is still widely used for prediction of temperature elevation during hyperthermia [4], [5]. Subsequent advances in computing technology and increased experimental data on human physiology helped researchers in developing better and more sophisticated human thermal models. In the 1960s, early versions of the well-known Wissler [6], Stolwijk [7], and Gagge [8] models were being developed. All later human thermal models for the most part, are probably extensions of these three mathematical models.

However, due to the natural complexity of human thermoregulation, it has been difficult to study the issue of accuracy for such models. Quantitative comparisons among models have also been difficult due to the

Manuscript received September 25, 2003. This research was supported by NASA grant NGT5-50444 from the Office of Biological and Physical Research (OBPR)

A. E. Iyoho and T. S. Jang are Ph.D students at the University of Missouri-Columbia, Columbia, MO 65211 USA (phone: 573-882-7799; fax: 573-884-5090; e-mail: aeie51@mizzou.edu or tsjx84@mizzou.edu)

S. S. Nair is the Associate Dean of Research in Engineering and Professor in the Mechanical and Aerospace Engineering department at the University of Missouri-Columbia, Columbia, MO 65211 USA (e-mail: nairs@missouri.edu)

individual characteristics of each model under particular environmental conditions [9]–[11]. From a user point of view, it has not been clear which of the models would be best suited for a particular environment and application. Various research teams [12]–[15] have developed models in the past decade to be used in environments that range from uniformly steady state to extremely transient and non-uniform. Models such as the Kansas State University model [14], [16], the Berkeley model [15], and the MU model [12] are in development to achieve such objectives. Even though these models incorporate more detail, they have their roots either in the Wissler [3] or the Stolwijk [7] models.

III. ADDITIONS TO THE 41-NODE MAN MODEL

The new human thermal model makes some additions to the 41-Node Man to improve the prediction of thermal comfort for an astronaut in space. The following sections outline additions made for the new model.

A. Two-dimensional Conduction

One-dimensional models cannot account for cases where disparate environmental conditions exist on different sides of the body. A study by Hall and Klemm showed that when the body was exposed to cold (-6.7°C) and hot (82ºC and 93.3°C) radiative temperatures on different sides of the body, skin temperature differences between the anterior and posterior sides ranged between 9-10ºC [17]. These experiments by Hall and Klemm were also validated through simulations of the two-dimensional model developed by Kuznetz where the environmental conditions of the experiments were duplicated for the simulations [18]. Kuznetz's model also predicted different anterior and posterior temperatures for the same body element. For wall temperatures of -6.7° and 82º C, temperature differences between Kuznetz's model and Hall and Klemm's experiment never exceed 1.5º C. A one-dimensional model where temperature does not vary with the angle cannot predict such temperature differences on different sides of the same body element.

B. Modeling the Digits

For the development of this model, explicit modeling of digits (fingers and toes) was incorporated, which has been suggested by NASA to be important. Studies have shown [19] that the digits, especially the fingers, respond to changes in the thermal environment quicker than all other locations of the body. Thus, a change in a digit temperature is a good indication of thermal imbalance in the body. Plus, digit modeling is needed to predict extremity discomfort in cold settings.

C. Detailed Cardiovascular Model

There is a need to incorporate a blood model that includes the explicit modeling of arteries and veins where blood temperature can vary at different areas in the body. In independently modeling arteries and veins, heat transfer occurs between the arteries and tissue, and between the veins and tissue. In addition, countercurrent heat exchange between arteries and veins approaches a realistic circulatory system.

D. AVA Modeling

The arteriovenous anastomoses are basically shunts which directly connect the arteries and venous plexuses. For heat exchange, most of this vasculature is located in the hands, feet, ears and hairless regions of the face. AVAs play an important role in thermoregulation. When they are open, large amounts of blood can pass through to the venous plexuses. It is estimated that blood flow into the subcutaneous venous plexuses can be as much as 30% of the total cardiac output [20]. Activation of sympathetic nerves leads to active vasoconstriction, and decrease in sympathetic activity leads to passive vasodilatation. In a moderately warm environment the AVAs are open. In a slightly cold environment, the AVAs are almost closed. The phenomenon termed cold induced vasodilation (CIVD) can be directly attributed to the AVAs. Thus, AVAs play a key role in regards to the thermal comfort of extremities. Due to the importance of AVAs in human thermoregulation, the functions of the AVAs are included in this model, and its inclusion paves the way for future studies involving extremity discomfort.

IV. MATHEMATICAL ANALYSIS

This model features three different clothing ensembles, nude, liquid cooling garment (LCG), and liquid cooling and ventilation garment (LCVG) with suit. For this paper, the nude case will be the focus in order to compare simulation results with existing experimental data. However, the complete documentation of the model, including parameter values (which are too numerous to mention), can be obtained if the reader desires further insight [12].

The human thermal system can be divided into two components. The first is the passive thermal system that includes non-decision making heat transfer processes. The second component is the active thermal system that includes all the decision-making processes such as sweating, shivering and vasomotor functions. These active systems attempt to update parameters or heat exchange rates on-line depending on the thermal state of the simulated subject.

A. Passive System

This human thermal model utilizes 14 cylindrical elements to represent the human body. Within each element are four concentric regions: the core, muscle, fat and skin layers. Each element contains radially and angularly varying temperature nodes. Each element contains six equally spaced angular sectors. Six angular sectors were used since it was stated that this enough to insure accurate temperature deviations in the angular direction [21]. Fig. 1 shows the nodal spacing within each sector for the nude case. For the nude case, there are a total of 686 temperature nodes. The heat equation for two-dimensional conduction and heat generation is shown below.

$$C\frac{\partial T}{\partial t} = Vk\left[\frac{\partial^2 T}{\partial r^2} + \frac{1}{r}\frac{\partial T}{\partial r} + \frac{1}{r^2}\frac{\partial^2 T}{\partial \theta^2}\right] + \dot{Q}_{blood} + \dot{Q}_{gen} + \dot{Q}_{resp} \quad (1)$$

The term on the left-hand side of (1) represents the heat storage, V represents the volume, C represents the thermal mass, and the bracketed term on the right represents the conduction between tissues. The last three terms on the right side represent the rate of heat addition due to blood, heat generation, and the respiratory system, respectively.

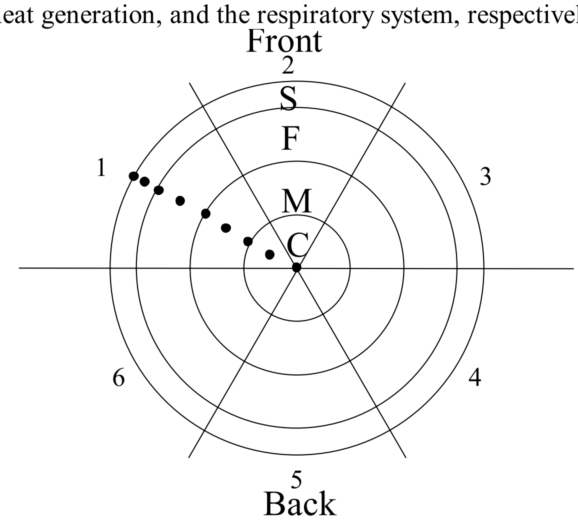

Fig.1 Cross-sectional view of an element and nodal spacing for the nude case.

Equation (1) is used for tissue nodes in the middle of a specific tissue region. However, there is a need for an equation for the temperature node at the interface between two distinct tissue regions. The following heat flux equality can be used for this purpose.

$$-k_{in}\frac{\partial T}{\partial r} = -k_{out}\frac{\partial T}{\partial r} \quad (2)$$

In (2), k_{in} represents the conductivity of the tissue layer on the inside of the interface and k_{out} represents the conductivity of the tissue layer on the outside of the interface.

In addition, at the edge of the skin layer, the following boundary condition must be imposed.

$$-k\frac{\partial T}{\partial r} = \dot{Q}''_{ext} \quad (3)$$

For the nude case

$$\dot{Q}_{ext} = \dot{Q}_{conv} + \dot{Q}_{rad} + \dot{Q}_{lat}, \quad (4)$$

where the last three terms represent the rate of heat transfer to due to convection, radiation and latent heat loss, respectively. Equations for convective and radiative heat loss for a cylinder are standard, and thus will not be included in this text.

Respiratory heat loss - The rate of respiratory heat loss has two components: sensible and latent heat loss such that

$$\dot{Q}_{resp} = \left(\dot{Q}_{resp,lat} + \dot{Q}_{resp,sens}\right)K_{resp}, \quad (7)$$

where

$$\dot{Q}_{resp,lat} = MR\frac{G_1}{T_{air,abs}}\left(Pv_{air} - Pg_{resp}\right), \quad (8)$$

and

$$\dot{Q}_{resp,sens} = \frac{Cp_{air}P_{air,abs}MR \cdot G_2}{T_{air,abs}}\left(T_{air} - T_{resp}\right), \quad (9)$$

where K_{resp} is the percentage of the respiratory heat loss at a specific temperature node, MR is the metabolic rate, $T_{air,abs}$ is the absolute air temperature, Pv_{air} is water vapor pressure of air, Pg_{resp} is the saturation pressure of water at the respiratory temperature, Cp_{air} is the specific heat of air, $P_{air,abs}$ is the absolute air pressure, T_{resp} is the respiratory temperature, and $G1$ and $G2$ are empirical constants .

Heat transfer due to blood - The rate of heat transfer due to the blood to each tissue node is

$$\dot{Q}_{blood} = hA_a(T_a - T) + (\dot{e}_b + hA_v)\left(T_v - T\right), \quad (10)$$

where $\dot{e}_b = \dot{m}_b Cp_b$, hA_a is the heat transfer coefficient between the tissue and artery, hA_v is the heat transfer coefficient between the tissue and vein, $\dot{e}_b$ is the thermal mass blood flow rate, and T_a and T_v are the artery and vein temperatures, respectively. In this model, blood flow is assumed to originate at the heart flowing to tissue layers through the arteries, which flow into the capillary bed and then exits the tissue layer through the veins. In this model, it is assumed that the blood entering tissue will exit the arteries approximately at the tissue temperature. Thus, blood entering the capillaries will approximately be at the tissue temperature. Thus, the term in (10) that involves $\dot{e}_b$ indicates perfect heat transfer within the capillary bed, or in other words that blood entering the capillary bed (at the tissue temperature) will exit at the vein temperature. Equation (10) was also used to model the heat transfer due to blood flowing through AVAs in the hands, feet and digits, where $\dot{e}_b$ represents the thermal mass blood flow rate through the AVAs.

B. Active System

The active thermal system used in this thermal model utilizes the equations used for sweating, shivering and vasomotor actions from the 41-Node Man [1].

Latent heat transfer - The latent transfer of heat from the skin is comprised of two components: diffusion and active sweating such that

$$\dot{Q}_{lat} = \dot{Q}_{dif} + \dot{Q}_{sweat}, \tag{11}$$

where $\dot{Q}_{dif} = AG_3\left(Pv_{air} - Pg_{skin}\right)^{-or\,0}$ and

$$\dot{Q}_{sweat} = -SK_{sweat}\,2^{(T-T_{set})_{skin}G_4}, \tag{12}$$

where

$$S = (T_c - T_{set})_{head}^{+or\,0}\left(G_5 + G_6\sum_{i=1}^{14}\gamma_{sw}(T_i - T_{set})_{skin}^{+or\,0}\right) \tag{13}$$

where A is the diffusion area, Pv_{air} is the water vapor pressure of the environment, Pg_{skin} is the saturated pressure of water at the skin temperature, K_{sweat} is the sweat distribution, T_{set} is the setpoint temperature, T_c is the core temperature, γ_{sw} is the skin mass distribution, and G_4, G_5 and G_6 are empirical constants. In addition, active sweating is limited by the maximum evaporative capacity

$$\dot{Q}_{\max} = \left(1 - \exp\left(-\frac{\dot{Q}_{sweat}G_7T_{air}R_w}{H_mAh_{fg,air}(Pg_{skin} - Pv_{air})}\right)\right) * \frac{H_{mass}Ah_{fg,air}(Pg_{skin} - Pv_{air})}{T_{air}R_w} \tag{14}$$

where H_{mass} is the mean mass transfer coefficient, $h_{fg,air}$ is the enthalpy of vaporization, R_w is the universal gas constant, and G_7 is an empirical constant. The superscript *"- or 0"* indicates that the preceding term must be either negative or zero and the superscript *"+ or 0"* indicates that the preceding term must be either positive or zero.

Shivering - The rate of heat production due to shivering is distributed within the muscle region of each element and is given by

$$\dot{Q}_{shiver} = \left(\sum_{i=1}^{14}(T_{set\,s} - T_s)_i^{+or\,0}\gamma_{sh,i}\right) * (T_{set\,c} - T_c)_{head}^{+or\,0}G_8K_{shiver}\frac{M_m}{M_{m0}}, \tag{15}$$

where $T_{set,s}$ is the skin setpoint temperature, T_s is the skin temperature, γ_{sh} is the skin mass distribution, $T_{set,c}$ is the core setpoint temperature, T_c is the core temperature, K_{shiver} is the shiver distribution, G_8 is an empirical constant and M_m/M_{m0} is the muscle mass to nominal muscle mass ratio. The superscript *"+ or 0"* indicates that the preceding term must be either positive or zero.

Vasomotor functions - In this model, the vasomotor actions work either to increase or decrease the blood flow rate to the skin. During vasodilation, the blood flow rate to the skin is increased to encourage heat loss to the environment. During vasoconstriction, the blood flow rate to the skin is decreased to inhibit heat transfer to the environment. Vasodilation occurs when the simulated subject is too warm, whereas vasoconstriction occurs when the simulated subject is cold. The skin thermal mass blood flow rate is updated on-line using the following equation:

$$\dot{e}_{b\to s} = \frac{\dot{e}_{b\to s,basal} + \dot{e}_{dil}}{1 + \Re}, \tag{16}$$

where $\dot{e}_{dil} = (T_c - T_{set\,c})_{head}^{+or\,0}G_9K_{dil}\frac{M_s}{M_{s0}}$ and

$$\Re = \left((T_{set\,c} - T_c)_{head}^{+or\,0} + \sum_{i=1}^{14}\gamma_{cons}(T_{set\,i} - T_i)_{skin}^{+or\,0}\right) * G_{10}K_{cons}\frac{M_s}{M_{s0}} \tag{17}$$

where K_{dil} is the vasodilation distribution, K_{cons} is the vasoconstriction distribution, M_s/M_{s0} is the skin mass to nominal skin mass ratio, and G_9 and G_{10} are empirical constants. The superscript *"+ or 0"* indicates that the preceding term must be either positive or zero.

V. RESULTS

A. Comparison with Hall and Klemm Experiments

The model was simulated using environmental conditions comparable to the experiments of Hall and Klemm [17]. For the simulation, the anterior and posterior sides of the body were exposed to 93.3 °C and –6.7 °C wall temperatures, respectively. The total simulation time was 30 minutes. The simulated subject was assumed to weigh about 70 kg with a 169 cm height. The subject was assumed to be resting, thus the metabolic rate was 81.4 W. The anterior temperatures were obtained by taking an average temperature of the frontal sectors (sectors 1-3). Similarly, the posterior temperatures were obtained by taking an average temperature of the rear sectors (sectors 4-6)

Fig. 2 show results that justify modeling two-dimensional heat flow. The desired outputs were the anterior and posterior skin temperatures of the arm. The results clearly show that the model can predict temperature variations on the same body element. As anticipated, the anterior side temperatures of each body element were greater than the posterior side temperatures.

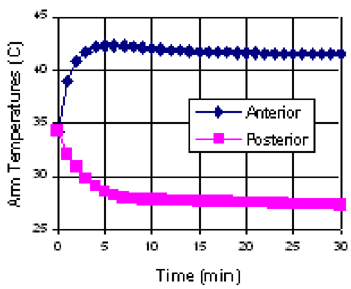

Fig. 2 Arm skin temperatures

Fig. 3 shows a comparison of predicted posterior skin temperatures with the experimental results of Hall and Klemm. The model tracks the experimental data fairly well with the difference in temperatures never exceeding 0.7 °C. In general, the model predicts cooler posterior skin temperatures than the experiment. This probably indicates that the model some what over-predicts the amount of heat loss due to active sweating.

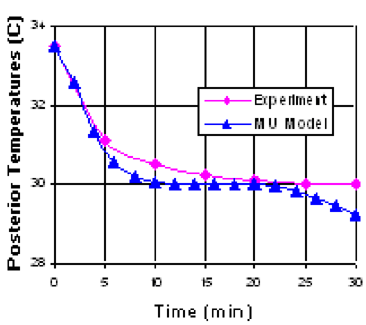

Fig.3 Comparison of MU Model predictions and experimental results for posterior skin temperature.

B. Comparison with Experiments Done by Grahn et al.

Grahn et al. hypothesized and then validated through experimentation that the recovery from mild hypothermia can be achieved quickly by mechanically distending blood vessels in the hand with subatomic pressure, and then applying heat [20]. They concluded that AVAs play a key role in this phenomenon in that applying subatomic pressure in conjuction with heat opens the AVAs to full capacity, which in turn allows a high blood flow through the venous plexuses in the hand. This blood is then heated and returns quickly to the core, thus somewhat directly heating the body core. The experiments conducted by Grahn et al. showed that their method resulted in a maximum rate of change in the external auditory meatus temperature (T_{EAM}) of 13.6 ± 2.1°C/h. This rate for the experimental group was 10 times faster than the maximum rate of the control group.

The MU Model was simulated in an attempt to predict the results of Grahn et al. to validate the AVA model formulated in this paper. The result of this simulation is shown in Fig. 4. Here, the predicted T_{EAM} of the MU Model is compared to that of a single experimental subject. The model shows good agreement with the experimental data, but more importantly the model predicted a maximum rewarming rate of 12.11°C/h, which also agrees well with the results found by Grahn et al.

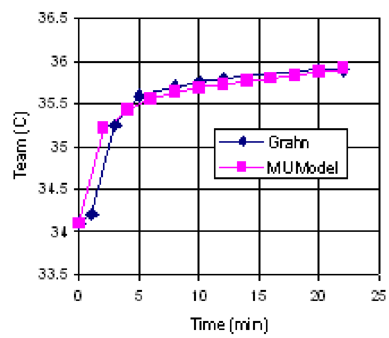

Fig.4 Comparison of MU Model predictions and experimental results for external auditory meatus temperature.

VI. CONCLUSIONS

A two-dimensional human thermal model was developed. The model included fingertip and toe temperature predictions along with countercurrent heat exchange involving arteries and veins. Arterial and venous countercurrent heat exchange is an especially nice feature in that it approaches a realistic representation of the human cardiovascular system especially when coupled with the modeling of the AVAs. In addition, the AVA model that was implemented was able to capture the phenomenon reported by Grahn et al. [20]. This is encouraging in that accurate AVA modeling will be needed when conducting extremity discomfort studies.

Results from simulations indicated that the model could also predict varying temperatures on a body segment due to disparate environmental conditions. This is especially important, because astronauts are exposed to disparate environmental conditions during extra-vehicular activity (EVA) in space. Thermal comfort must be insured even in thermally disparate environments.

We are presently working on improving the following features, now that the basic model has been successfully developed: shivering and sweating functions, heat transfer coefficients used in the cardiovascular model; better distribution of the AVA models throughout the body; effects of fluid shifts due to microgravity. Validations of the models will also be performed using a human thermal facility in our laboratory and will be included in the final version of the paper.

REFERENCES

[1] G.C. Bue, *Computer Program Documentation: 41-Node Transient Metabolic Man Program*. Houston, TX: Lockheed Engineering and Sciences Company. LESC-27578, a.ka. CTSD-0425, 1989.

[2] H.H. Pennes, "Analysis of tissue and arterial blood temperatures in the resting human forearm", *J. Appl. Physiol*., 1, 1948, pp 93-122.

[3] E.H. Wissler, "Mathematical simulation of human thermal behavior using whole body models", In: *Heat Transfer in Medicine and Biology*, ed. Avraham, Shitzer and Robert C. Eberhardt, 1:325-373. New York: Plenum Press, 1985.

[4] R. K. Jain, "Temperature distributions in normal and neoplastic tissues during normothermia and hyperthermia," Annals of the New York Academy of Sciences, vol. 335, pp. 98-106, 1980.

[5] R. B. Roemer and T. C. Cetas, "Application of bioheat transfer simulations to hyperthermia," Cancer Research, vol. 44, pp. 4788s-4798s, 1984.

[6] E. H. Wissler, "A mathematical model of the human thermal system," Bulletin of Mathematical Biophysics, vol 26, pp. 147-166, 1964.

[7] J.A. Stolwijk, *A Mathematical Model of Physiological Temperature Regulation in Man.* Washington, D.C.: NASA CR-1855, 1971.

[8] A.P. Gagge, "A two-node model of human temperature regulation in fortran", *Bioastronautics Data Book*, J.F. Parker, Jr. and V.R. West (editors), NASA SP-3006, Washington, D.C., 1973, pp. 142-148.

[9] C.G. Crandall, J.M. Johnson, V.A. Convertino, P.B. Raven, and K.A. Engelke, "Altered thermoregulatory responses after 15 Days of head-down tilt, *J. Appl. Physiol*., 77(4), 1994, pp 1863-1867.

[10] R. A. Haslam and K. C. Parsons, "Computer-based models of human responses to the thermal environment: Are their predictions accurate enough for practical use?," in Thermal Physiology, J.B. Mercer, Ed., 1989, pp. 763-768.

[11] C. L. Hwang and S. A. Konz, "Engineering models of the human thermoregulatory system: a review," IEEE Transactions on Biomedical Engineering, vol. 24(4), pp. 309-325, July 1977.

[12] A.E. Iyoho, *The Development of a 2-D Human Thermal Model for EVA Applications*, University of Missouri-Columbia, MS Thesis, 2002.

[13] J. D. French, A. D. Viswanath, S. S. Nair, J. B. Miles and C. H. Lin, "Parameters and assumptions in human thermal modeling for EVA applications," SAE Transactions, Journal of Aerospace, vol. 106, pp. 579-586, SAE 972320, 1997.

[14] G. Fu, *A Transient, Three-Dimensional Mathematical Thermal Model for the Clothed Human*, Ph.D. Thesis, Kansas State University, 1995.

[15] C. Huizenga, H. Zhang and E. Arens, " A model of human physiology and comfort for assessing complex thermal environments," Building and Environment, vol. 36, pp. 691-699, 2001.

[16] F. Hsu, *Modeling, Simulation, and Optimal Control of the Human Thermal System*, Ph.D. Thesis, Kansas State University, 1971.

[17] J.F. Hall and F.K. Klemm, "Thermoregulatory Responses in Disparate Thermal Environments", *J. Appl. Physiol.* 23(4), 1967, pp 540-544.

[18] L.H. Kuznetz, "A two-dimensional transient mathematical model of human thermoregulation", *American Journal of Physiology*, 237(5), 1979, pp R266-R277.

[19] V.S. Koscheyev, S. Paul, G.R. Leon, D. Tanchida, T.J. Taylor and I.V. Koscheyev, "Body surface temperature tuning as a comfort support system in space and other extreme environments", *SAE Technical Paper Series*, 1998.

[20] D. Grahn, J.G. Brock-Utne, D.E. Watenpaugh, and H.C. Heller, "Recovery from mild hypothermia can be accelerated by mechanically distending blood vessels in the hand", *J. Appl. Physiol*., 85, 1998, pp 1643-1648.

[21] T. Mungcharoen, *A Two-Dimensional Human Thermal Model for Execution on a Parallel Processor*, University of Texas-Austin, Ph.D Dissertation, 1989.